Development 127, 1607-1616 (2000)
Printed in Great Britain © The Company of Biologists Limited 2000
DEV4300

Fate of the mammalian cardiac neural crest

Xiaobing Jiang[1,3], David H. Rowitch[4,*], Philippe Soriano[5], Andrew P. McMahon[4] and Henry M. Sucov[2,3,‡]

Departments of [1]Biological Sciences and [2]Cell & Neurobiology, [3]Institute for Genetic Medicine, Keck School of Medicine, University of Southern California, 2250 Alcazar St., IGM 240, Los Angeles, CA 90033, USA
[4]Department of Molecular and Cell Biology, Harvard University, 16 Divinity Ave., Cambridge, MA 02138, USA
[5]Program in Developmental Biology, Division of Basic Sciences, A2-025, Fred Hutchinson Cancer Research Center, 1100 Fairview Avenue North, PO Box 19024, Seattle, WA 98109, USA
*Present address: Department of Pediatric Oncology, Dana Farber Cancer Institute, 44 Binney St., Boston, MA 02115, USA
‡Author for correspondence (e-mail: sucov@hsc.usc.edu)

Accepted 26 January; published on WWW 21 March 2000

SUMMARY

A subpopulation of neural crest termed the cardiac neural crest is required in avian embryos to initiate reorganization of the outflow tract of the developing cardiovascular system. In mammalian embryos, it has not been previously experimentally possible to study the long-term fate of this population, although there is strong inference that a similar population exists and is perturbed in a number of genetic and teratogenic contexts. We have employed a two-component genetic system based on Cre/lox recombination to label indelibly the entire mouse neural crest population at the time of its formation, and to detect it at any time thereafter. Labeled cells are detected throughout gestation and in postnatal stages in major tissues that are known or predicted to be derived from neural crest. Labeling is highly specific and highly efficient. In the region of the heart, neural-crest-derived cells surround the pharyngeal arch arteries from the time of their formation and undergo an altered distribution coincident with the reorganization of these vessels. Labeled cells populate the aorticopulmonary septum and conotruncal cushions prior to and during overt septation of the outflow tract, and surround the thymus and thyroid as these organs form. Neural-crest-derived mesenchymal cells are abundantly distributed in midgestation (E9.5-12.5), and adult derivatives of the third, fourth and sixth pharyngeal arch arteries retain a substantial contribution of labeled cells. However, the population of neural-crest-derived cells that infiltrates the conotruncus and which surrounds the noncardiac pharyngeal organs is either overgrown or selectively eliminated as development proceeds, resulting for these tissues in a modest to marginal contribution in late fetal and postnatal life.

Key words: Neural crest, Fate, Mammal, Cardiac development, Cre recombinase, Outflow tract

INTRODUCTION

In all vertebrate embryos, the heart initially forms as a single linear tube located along the ventral midline. Blood flow from the early heart is carried from the primordial ventricle through a single outflow vessel, known as the truncus arteriosus. This vessel bifurcates in a region termed the aortic sac into a series of bilaterally paired pharyngeal arch arteries that connect to bilaterally paired dorsal aortae. As development proceeds, a series of morphogenic processes result in the division of the single outflow vessel to become the ascending aorta and pulmonary trunk (Fananapazir and Kaufman, 1988), and in the asymmetric reorganization of the pharyngeal arch arteries to become the left-sided arch of the aorta and associated blood vessels (Wilson and Warkany, 1949).

The neural crest is a migratory population of cells that originate from the dorsal aspect of the neural tube. Neural crest cells form at all axial levels of the embryo, and assume a variety of ectodermal and mesodermal fates as they reach peripheral locations (LeDouarin, 1982; Hall and Horstadius, 1988). A variety of experimental approaches indicate that a specific crest cell population, termed the cardiac neural crest, is responsible for morphogenesis of the outflow region of the developing heart. In avian embryos, where the role and fate of the cardiac neural crest is particularly well established, removal of the dorsal neural tube (including the neural crest precursors) between the otic vesicle and the third somite results in a persistent single outflow vessel, a phenotype termed persistent truncus arteriosus, and in a variety of defects in the organization of the derivatives of the pharyngeal arch arteries (Kirby et al., 1983; Kirby and Waldo, 1990).

Fate mapping of the avian cardiac neural crest has been facilitated by the ability to transplant and identify the cellular derivatives of corresponding domains of the dorsal neural tube between chick and quail embryos (LeDouarin, 1982; Le Lievre and LeDouarin, 1975; Miyagawa-Tomita et al., 1991). Avian crest cells initially envelop the endothelium of the caudal pharyngeal arch arteries as they migrate ventrally within each pharyngeal arch. Two prongs of crest cells then extend into the aortic sac and initiate the formation of the aorticopulmonary

septum, which contributes to the formation of distinct pulmonary and aortic structures (Waldo et al., 1998). The ultimate fate of this portion of the avian cardiac neural crest is to form the smooth muscle lining of the blood vessels around which they assemble, and to contribute to the outflow valves.

The thymus, thyroid and parathyroid glands form from the pharyngeal system in proximity to the outflow region of the heart. A role for the cardiac neural crest population in the morphogenesis of these organs in avian embryos has been inferred from hypoplastic deficiencies in these organs following neural crest ablation (Bockman and Kirby, 1984; Kirby and Waldo, 1990).

The fate of the mammalian cardiac neural crest is only poorly defined. In mouse and human embryos, a number of genetic (Greenberg, 1993; Franz, 1989; Epstein et al., 1991; Lee et al., 1997; Kurihara et al., 1995b) and teratogenic (Wilson and Warkany, 1949; Lammer et al., 1985) manipulations result in defects such as persistent truncus arteriosus, aortic arch artery abnormalities, and/or thymic, thyroid or parathyroid deficiencies. The spectrum of these malformations so closely resembles those seen in neural-crest-ablated avian embryos that it has long been inferred that there is a mammalian equivalent to the avian cardiac neural crest and that these manipulations interfere with some aspect of mammalian cardiac neural crest biology. However, it has not been possible in mammalian embryos to label neural crest cells, either by transplantation or injection, in a manner that allows long-term survival of the recipient embryo. Injection of lineage tracers into mammalian embryos ex utero (Serbedzija et al., 1992) or cultured in vitro (Fukiishi and Morriss-Kay, 1992) has demonstrated that neural crest cells populate the pharyngeal arches in a manner similar to avian embryos, but these do not provide sufficient cell labeling or allow embryonic survival to demonstrate the behavior of crest cells in the morphogenesis of the outflow region of the heart. A number of molecular markers, both endogenous (Conway et al., 1997) and transgenic (Lo et al., 1997; Liu et al., 1994; Means and Gudas, 1997), have been useful in marking the initial population of migratory cardiac neural crest, but most suffer from either being no longer expressed at stages after occupancy of the pharyngeal arches, and/or from ectopic sites of expression such that expression does not necessarily correlate with a neural crest cell origin. A transgenic line in which β-galactosidase is expressed from the connexin 43 promoter (Lo et al., 1997) has to date been the most reliable marker of mammalian cardiac neural crest cell fate (Waldo et al., 1999), but expression of this transgene is extinguished in mid to late gestation. Furthermore, all of these molecular markers are potentially subject to altered expression patterns after genetic or teratogenic manipulation, making their use in defining crest cell fate in an experimental context less reliable.

The ideal marker of neural crest cell fate would completely and exclusively mark the crest cell population, would be detectable at the time of crest cell formation and migration, would remain detectable for the lifetime of the cell, and would be unaffected by experimental manipulation. The quail-chick chimeric avian embryo achieves these criteria by virtue of a nuclear morphology that is cytologically distinguishable between the two species. For mammalian studies, we have utilized a two-component system based on Cre/lox recombination to indelibly mark the neural crest cell lineage in mice by gene expression. One component is a transgene expressing Cre recombinase under the control of the *Wnt1* promoter and enhancer (Danielian et al., 1998). The *Wnt1* gene is expressed specifically in the neural plate, in the dorsal neural tube and in the early migratory neural crest population at all axial levels excluding the forebrain. Expression of *Wnt1* is extinguished as the crest cell lineage migrates away from the neural tube, and is not expressed at any other time or in any other place during development or in postnatal life (Echelard et al., 1994). The second component is a conditional reporter gene termed R26R that expresses β-galactosidase from the ROSA26 locus only upon Cre-mediated recombination (Soriano, 1999). The ROSA26 locus has been shown to be ubiquitously and uniformly expressed at all developmental and postnatal times, and has no apparent sensitivity in expression to genetic or environmental manipulation (Friedrich and Soriano, 1991; Zambrowicz et al., 1997). Without recombination, the transcript originating from the ROSA26 promoter encodes an irrelevant sequence, whereas after Cre-mediated recombination, the transcript produces a functional β-galactosidase protein. Importantly, the progeny of cells that have undergone recombination will continue to be β-galactosidase positive, even though the Wnt1-Cre transgene is no longer active. Although still potentially subject to artifactual results, we demonstrate that all known neural crest cell lineages are efficiently and stably marked by combining these two components, and have used this system to define the long-term fate of the cardiac neural crest lineage. In the accompanying paper (Chai et al., 2000), a similar analysis of craniofacial neural crest contribution to tooth and mandibular formation is presented.

MATERIALS AND METHODS

The Wnt1-Cre transgenic line (Danielian et al., 1998) was constructed by introduction of a cassette expressing cytoplasmic Cre recombinase into the *Wnt1* promoter/enhancer construct pWEXP3C. Fidelity of expression was confirmed by in situ hybridization at E10.5 (data not shown). The R26R conditional reporter allele (Soriano, 1999) was made by homologous recombination of a gene trap cassette into a 5′ intron of the ROSA26 locus (Friedrich and Soriano, 1991); the gene trap cassette contains (from 5′ to 3′) a splice acceptor, a *loxP* site, a neomycin coding sequence followed by a polyadenylation sequence, a second *loxP* site and a *lacZ* coding sequence followed by a polyadenylation element. Mice were maintained on a 0600 to 1800 hours light-dark cycle, with noon of the day of observation of a vaginal plug defined as E0.5. Our embryos appear to be 0.25-0.5 days more developmentally advanced relative to those of the same nominal age described by Kaufman (1992).

Embryos isolated at E9.5 and 10.5 were X-gal stained in whole mount by standard procedures, then paraffin embedded and sectioned at 5 μm thickness. We experienced only partial stain penetration in embryos at E10.5, so that sections from these embryos were photographed under dark-field illumination, where the lower amount of X-gal product is more apparent and appears pink. Embryos isolated at later stages and newborn pups were cryopreserved in increasing sucrose solutions, culminating in a 50:50 mix of 30% sucrose:OCT, then frozen in OCT. In most cases, infiltration of OCT was facilitated by removal of all abdominal structures posterior to and including the diaphragm, and by dissection of the thoracic cavity to expose the heart. 20 μm cryostat sections were fixed and X-gal stained by standard procedures. All sections were counterstained with eosin and nuclear fast red. Adult tissues were isolated by dissection. For frozen

sections, tissue was processed exactly as above. For whole-mount staining, the heart and adjacent vessels were trimmed of noncardiac tissue. The tissue was fixed and stained as above for whole-mount embryos, except that interior rinsing, fixation and staining were facilitated by manual perfusion through a 30-gauge needle inserted into the left and right ventricular chambers, and into the openings of peripheral arteries. Adrenal tissue was bisected manually before fixation and whole-mount staining.

RESULTS

Specificity of reporter gene expression in *Wnt1-Cre/R26R* embryos

By crossing the *Wnt1-Cre* transgene with the *R26R* allele, we have obtained a series of embryos and postnatal animals that were stained to reveal β-galactosidase-positive cells. Based on prior avian and mammalian studies, we expected that labeled cells, indicative of a neural crest cell origin, would be found in a number of tissues throughout embryonic and postnatal stages, such as dorsal root ganglia, peripheral nervous system, melanocytes, adrenal medulla (Fig. 1) and craniofacial mesenchyme (see below and the accompanying paper (Chai et al., 2000)). These tissues were all labeled extensively, if not completely, suggesting that recombination of the R26R reporter gene driven by the *Wnt1-Cre* transgene is close to if not completely efficient at all axial levels. Furthermore, there was a complete absence of ectopic expression in ectodermal epithelium, endoderm, endothelium, notochord and paraxial mesoderm at all stages.

In the pharyngeal region, whole-mount staining of embryos at E9.5 (Fig. 1A) and E10.5 (not shown) revealed extensive labeling of cells in the pharyngeal arches. In sections (Fig. 2), the entire mesenchymal component of each arch is labeled, whereas the pharyngeal ectoderm, endoderm and vascular endothelium are unlabeled. There was essentially complete labeling of presumptive neural-crest-derived mesenchymal cells in all pharyngeal arches, including arches 3, 4 and 6, which are the domain of the cardiac neural crest, as well as in the first and second arches. The small number of unlabeled mesenchymal cells within each arch are most likely myoblasts and endothelial cells, which are not of neural crest origin.

Migration of cardiac neural crest cells to the heart

The outflow tract of the early heart is initially located immediately ventral to the endodermal foregut. At E9.5, blood flow from the heart is primarily routed through the second and third pharyngeal arch arteries; the first arch artery is in the process of regression. The mesenchyme of pharyngeal arches four and six is present, although the fourth and sixth arch arteries have not yet formed. At this time, neural crest cells can be observed surrounding the second and third pharyngeal arch arteries (Fig. 2A,C). Neural crest cells do not envelop the dorsal aortae, but rather lie lateral to these vessels where the pharyngeal arch arteries originate. Initially, a thin layer of neural crest cells becomes interposed between the foregut and the aortic sac, which increases in number of cells as development proceeds; it is unclear if this increase is a result of the accumulation of additional migratory cells into the ventral foregut region, or of cell division, or of a combination of the two. Labeled cells are also seen at E9.5 migrating within the lateral walls of the aortic sac and the truncus arteriosus, immediately adjacent to the outflow tract endothelium, but are not yet seen within the conus arteriosus (Fig. 2B,C).

Distribution of crest cells during the formation of the outflow tract septa

During the E10.5-11.5 period in the mouse embryo, several important changes in the organization of the outflow region are underway. The process of heart looping causes the outflow tract to originate from the future right ventricle, the second pharyngeal arch arteries regress during this period, and the fourth and sixth arch arteries form connections to the aortic sac. Two contiguous septa, the aorticopulmonary septum distally and the conotruncal septum proximally, are beginning to form, which will ultimately divide the outflow tract into aortic and pulmonary outflow vessels, concurrently forming the outflow valves and the subvalvular (ventricular) component of the mature outflow tracts. The organization of the pharyngeal arch arteries through E11.5 remains highly symmetrical, although the outflow tract septa show asymmetry as they begin to form (see below).

Labeled mesenchymal cells continue to occupy the pharyngeal arches and surround the pharyngeal arch arteries during this period. Furthermore, the distribution of labeled cells around the pharyngeal arch arteries remains bilaterally symmetric through E11.5 (Figs 2E-H, 3A,B). There is no apparent alteration in the pattern of crest cell distribution around the second pharyngeal arch arteries, either with respect to earlier time points or with respect to the pattern around the third arch arteries, that might account for the regression of these vessels. At E10.5, neural crest cells completely constitute the subendothelial tissue of the truncus arteriosus and can now

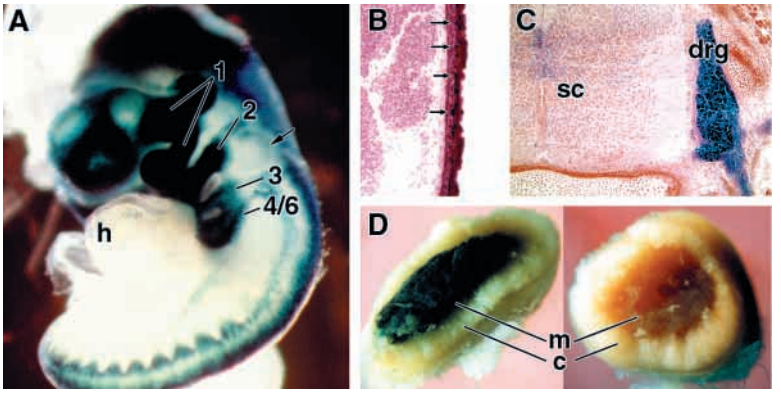

Fig. 1. Specificity and efficiency of neural crest marking by the Wnt1-Cre and R26R genes. (A) Whole-mount staining of a E9.5 embryo. Labeling is seen in the pharyngeal arches (numbered), dorsal neural tube and migratory neural crest in the trunk. The heart (h) is unlabeled, but is in obvious proximity to the pharyngeal arches. The arrow indicates the otic vesicle. (B,C) Staining in a E15.5 embryo. The arrows in B point to labeled cells scattered in the epidermal layer, which are presumptive melanocytes, and C illustrates a dorsal root ganglion (drg) lateral to the spinal cord (sc). (D) Staining of adrenal tissue from a Wnt1-Cre/R26R adult (left) and a nontransgenic control adult (right). Only the adrenal medulla (m) is labeled, and not the adrenal cortex (c).

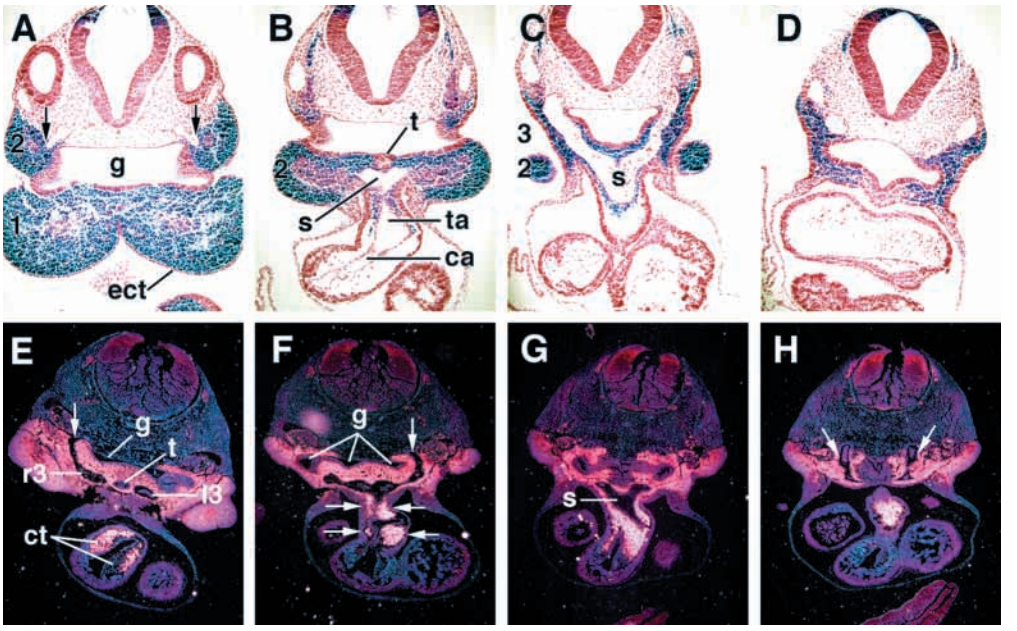

Fig. 2. Initial migration of neural crest into the heart. (A-D) Serial sections of an embryo at E9.5, taken at the level of the first pharyngeal pouch and the origins of the second pharyngeal arch arteries (A), the second pharyngeal pouch (B), the third pharyngeal arch arteries (C), and at the third pharyngeal pouch (D). Numbers indicate pharyngeal arches. Note the extensive labeling of pharyngeal arch mesenchyme, but not ectoderm, foregut endoderm or vascular endothelium. Neural crest cells can be seen populating the truncus arteriosus in B,C, but not the cushions of the conus arteriosus. The arrows in A point to the junction between the dorsal aortae (surrounded by unlabeled cells) and the second arch arteries (surrounded by labeled cells). The thyroid diverticulum is apparent in B at the ventral floor of the second pharyngeal pouch. (E-H) Sections of whole-mount stained embryos at E10.5. These images were photographed in dark field, where the X-gal product appears pink (see Methods). Sections shown are at a level slightly anterior to the origins of the third arch arteries from the aortic sac (E), at the origins of the fourth arch arteries from the aortic sac (F), slightly posterior to the origins of the fourth arch arteries from the aortic sac (G), and at the level of the origins of the sixth arch arteries from the dorsal aortae (H). The vertical arrows in E, F and H point to the junction between the dorsal aortae (surrounded by unlabeled cells) and the third, fourth and sixth arch arteries (surrounded by labeled cells). Labeled cells surround the thyroid (E), constitute the entirety of the mesenchyme of the truncus arteriosus in F (indicated by horizontal arrows) and G, and are invading into the conus cushions in E. r3 and l3 identify the right and left third arch arteries. Abbreviations: ca, conus arteriosus; ct, conotruncus; ect, pharyngeal ectoderm; g, foregut; s, aortic sac; t, thyroid; ta, truncus arteriosus.

be seen also invading the conal cushions (Fig. 2E-G); a similar yet more advanced pattern is seen at E11.5 (Fig. 3A). The conotruncal cushions are not completely composed of labeled cells, as is expected since a population of cushion cells is known to originate by mesenchymal transformation of the adjacent endothelium (Nakajima et al., 1994), and later by the introduction of myocytes (van den Hoff et al., 1999). However, it is clear that the neural crest contributes substantially to the conotruncal cushion mesenchyme.

The outflow tract septa are organized in a spiral manner, such that when outflow tract septation is completed, the aorta and pulmonary trunk rotate 180˚ around their common longitudinal axis. Histologically, this organization is evident at E10.5 by the projection of the aorticopulmonary septum into the lumen of the aortic sac where this compartment penetrates the posterior body wall. At E10.5, labeled cells of presumptive neural crest origin completely constitute the nascent aorticopulmonary spiral septum (Fig. 2F,G). However, even at E11.5, when overt septation is established, the distribution of crest cells within the truncus arteriosus and aortic sac is still remarkably bilaterally symmetric (Fig. 3A).

Distribution of neural crest cells during asymmetric reorganization of the outflow region

The asymmetric nature of the reorganization of the outflow vessels is first apparent at E12.0. The most obvious manifestation of this reorganization is in the dissolution of most of the right sixth aortic arch artery, and the extension of the aorticopulmonary septum as a wedge of tissue between the left fourth and sixth arch arteries. The abundance of labeled cells, which previously surrounded the right sixth arch artery at earlier stages, is no longer present at E12.0 (Fig. 3D; compare with 3B), whereas heavy labeling persists around the left 6th artery. We cannot yet determine whether this asymmetry in labeling pattern arises from cell death specifically on the right side, or from migration of cells to the left side or to more anterior positions. Bilaterally symmetric labeling is still observed around the left and right third and fourth arch arteries (Fig. 3C; compare with 3A).

By E12.0, the single outflow vessel seen at earlier stages is definitively septated, at least over much of its length. The pulmonary trunk connects to the left sixth arch artery and the ascending aorta connects to the left and right fourth and third arch arteries. In the posterior body wall, a broadly distributed mass of labeled mesenchymal cells completely surrounds these vessels (a pattern established earlier as the aortic arch arteries first formed). Labeled mesenchymal cells also project in an unbroken stream through the conotruncal region, up to the junction of the conus with the wall of the right ventricle (Fig. 3C). However, a significant alteration in the distribution pattern of labeled cells in the forming aorticopulmonary and conotruncal septa is first seen at E11.5-12.0. Whereas, at earlier stages, the neural crest derivatives were widely distributed within the conotruncal cushions, as these cushions fuse to form the conotruncal septum, the neural-crest-derived cells become localized in a thin subendothelial layer along the seam of fusion (Fig. 3C). In regions where the conotruncal cushions have not yet fused, a broadly distributed mass of labeled cells can be seen populating the cushion mesenchyme, similar to earlier stages (e.g., Fig. 4A). This process also occurs in the

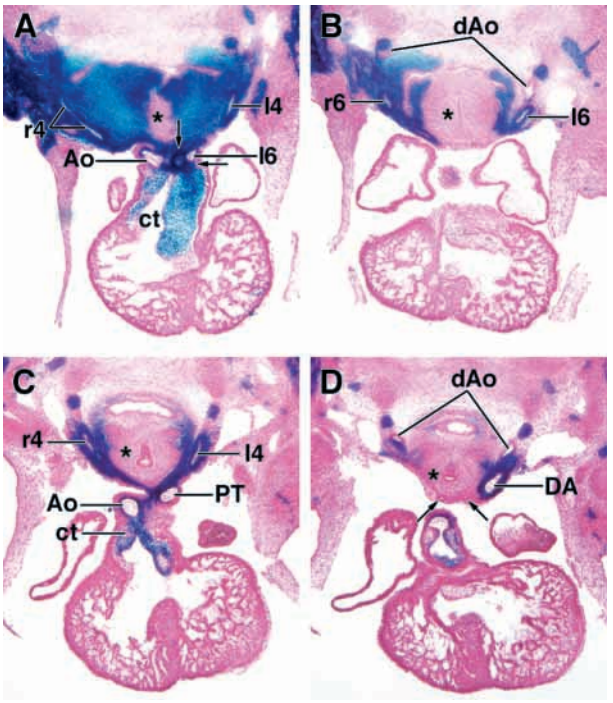

Fig. 3. Distribution of neural crest during aorticopulmonary and conotruncal septal formation. Sections shown are from an embryo at E11.5 (A,B) and at E12.0 (C,D). At E11.5, a mass of labeled mesenchyme surrounds the left and right fourth (A) and sixth (B) arch arteries. The staining pattern is symmetric in this embryo, but the sectioning was slightly off-angle. Labeled cells forming the aorticopulmonary septum (indicated by two arrows in A) which separates the outflow tract into the nascent aorta and pulmonary trunk at the origin of the left sixth arch artery, and diffuse cells in the conotruncal cushions are evident. At E12.0, the left and right fourth arch arteries are still surrounded by labeled mesenchymal cells (C), as is the left sixth arch artery (now known as the ductus arteriosus; D), whereas the right sixth arch artery has regressed and no labeled cells are evident between the right dorsal aorta and the outflow tract of the heart ventral to the splanchnic mesoderm of the trachea. The small patch of labeled cells in D ventral to the right dorsal aorta is a component of the mesenchyme that surrounds the right fourth arch artery seen in C. Labeled cells in the aorticopulmonary septum at E12.0 are present at the seam between the aorta and pulmonary trunk, and labeled cells in the conotruncal cushions are subendothelially localized as fusion of the conotruncal septum occurs. The arrows in D point to the pulmonary arteries, which are unlabeled. The asterisk in all panels identifies the splanchnic mesoderm that surrounds the trachea. Abbreviations: Ao, ascending aorta; ct, conotruncus; DA, ductus arteriosus; dAo, dorsal aorta; PT, pulmonary trunk; l4, l6, r4, r6, left and right fourth and sixth pharyngeal arch arteries.

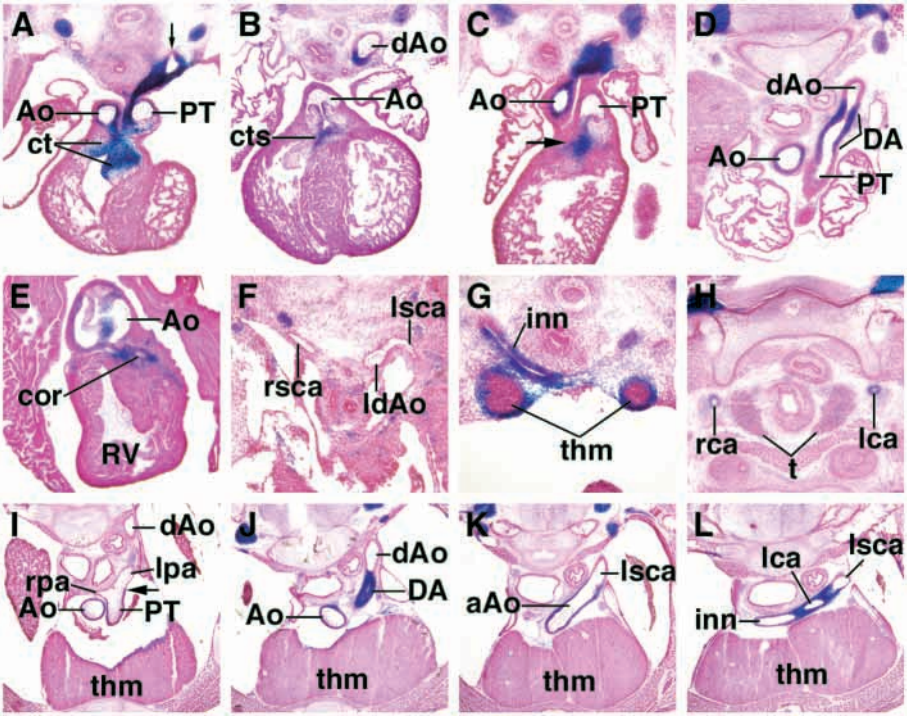

Fig. 4. Distribution of neural crest progeny during cardiac maturation. Sections shown are from embryos at E11.5 (F), E12.5 (A), E13.5 (B,G), E14.5 (C) and E15.5 (D,H), and from a newborn (12 hour) pup (E,I-L). The sections in A and C lie between the ductus arteriosus and the arch of the aorta, and in B lies just beneath the ductus arteriosus; the dark wedge of labeled cells ventral to the dorsal aorta will be incorporated into either vessel wall. The arrow in A indicates the dorsal aorta at the junction with the ductus arteriosus. Cells are also apparent in the conotruncal region, as the septum forms (A), in the immediate subvalvular region of the conotruncal septum (B,C), and in the aortic valve leaflets (B). (D) The near complete representation of labeled cells in the wall of the ductus arteriosus, whereas labeled cells are present only subendothelially in the ascending aorta and pulmonary trunk, and are not seen in the dorsal aorta. (E) A section through the aortic valve and the right ventricle of a newborn pup, with labeled cells contributing to the postnatal valve leaflets and to tissue around the origin of a coronary artery. (F) The origins of the subclavian arteries at a caudal (nonpharyngeal) thoracic level at E11.5. No labeled cells surround these vessels, at this time or when these vessels ascend anteriorly. (G) The thymic lobes surrounded by labeled cells at E13.5, adjacent to the innominate artery (inn). (H) The absence of appreciable staining in the maturing thyroid at E15.5, although the walls of the carotid arteries (rca, lca) are labeled. (I-L) Serial sections at ascending levels from a newborn pup. The staining pattern seen at earlier stages, including the subendothelial layer of labeled cells seen around the ascending aorta, pulmonary trunk and arch of the aorta, the absence of staining around the pulmonary arteries, the dorsal aorta and the left subclavian artery, and the extensive staining around the ductus arteriosus are still apparent at birth. The arrow in I indicates the transition from the pulmonary trunk (labeled) to the left pulmonary artery (unlabeled). The section of L is immediately anterior to the arch of the aorta, at the origin of the innominate and left carotid arteries. Abbreviations: Ao, ascending aorta; aAo, arch of the aorta; cor, coronary artery; ct, conotruncus; cts, conotruncal septum; DA, ductus arteriosus; dAo, dorsal aorta; inn, innominate artery; lca, left carotid artery; ldAo, left dorsal aorta; lpa, left pulmonary artery; lsca, left subclavian artery; PT, pulmonary trunk; rca, right carotid artery; rpa, right pulmonary artery; rsca, right subclavian artery; RV, right ventricle; t, thyroid; thm, thymus.

proximal portion of the aortic sac (Fig. 3C) such that, after E12.0, the vessel walls of the ascending aorta and pulmonary trunk immediately distal to the outflow valves are mostly (although not completely) composed of unlabeled cells, presumably derived from the outer mesothelial lining of earlier stages. Thus, it appears that the mass of neural-crest-derived cells that constitute the early aorticopulmonary and conotruncal mesenchyme mostly die or are overgrown as septal formation is completed.

Distribution of neural crest cells in the mature cardiovascular system

The general pattern of distribution of neural-crest-derived cells seen at E12.0 remains mostly unchanged as development proceeds and in the postnatal period, in spite of significant alterations in the organization of the outflow region of the heart.

The relationship between the ascending aorta and the third and fourth arch arteries becomes modified as the left fourth arch artery becomes the arch of the aorta and the left third arch artery becomes the left carotid artery, and as the innominate artery forms from a region of the aortic sac between the right third and fourth arch arteries. Where a mass of labeled mesenchymal cells surrounded these vessels in the earlier stages (prior to E12.0), this pattern continues in the mature arteries but the broad distribution of labeled mesenchymal cells becomes concentrated within the smooth muscle layer around the vessel wall, with an apparent absence of labeled mesenchymal cells in more peripheral locations (not shown; see also Fig. 4G,H,L). As noted above, we cannot define whether this concentration occurs by cell death in regions more distal to the vessel wall, or by recruitment of the peripheral cells into more proximal positions. However, the expansion of the splanchnic mesoderm population surrounding the forming trachea (e.g., Fig. 3) must in part contribute to the exclusion of neural-crest-derived mesenchymal cells in the region of the foregut. Relative to the other vessels, the ductus arteriosus, which is derived from the distal portion of the left sixth arch artery, retains a much thicker column of labeled cells around its wall in late-stage embryos (Fig. 4D) and even in the newborn animal (12 hours postparturition; Fig. 4J). The ductus arteriosus closes in the postnatal period, becoming transformed into a ligament known as the ligamentum arteriosum. In the adult, most of the ligamentum arteriosum is composed of labeled cells (Fig. 5A,C), reflective of their sixth arch neural crest derivation.

The dorsal aortae in the early embryo are not surrounded by neural crest cells (Figs 2, 4F), and the mature vessel derivatives of the dorsal aortae are not labeled in later embryos or postnatally (Fig. 5A). Anteriorly, the carotid arteries form bilaterally from the third arch arteries (proximal to the arch of the aorta) and from the dorsal aortae (more distal). In late embryos and postnatally, the proximal portions (in the thoracic region) of both carotid arteries retain staining (Figs 4H,L, 5A,F), reflective of the investment of the third aortic arch arteries by third arch neural crest, whereas cranial regions of the carotid arteries are not labeled (not shown), reflective of the origin of these portions of the vessels from the dorsal

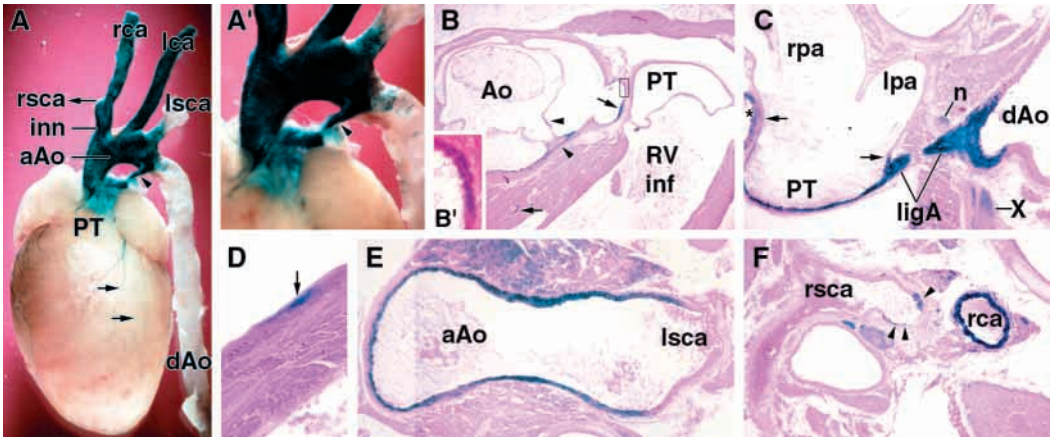

Fig. 5. Ultimate fate of the cardiac neural crest. (A) Distribution of labeled cells in a 7 week adult heart stained in whole mount (A′ is a higher magnification of A). Note the extensive staining in the ascending aorta and the arch of the aorta, in the innominate and left and right carotid arteries, but not in the dorsal aorta or in the left subclavian artery except for scattered cells near the arch of the aorta. The ligamentum arteriosum (indicated by the arrowhead) is heavily stained. The right subclavian artery was torn away from the innominate artery during dissection, but its location is indicated by the leftward-pointing arrow. The labeled structures on the ventricular surface are nerve fibers (see also D). (B-F) Distribution of labeled cells in sections of a 9-week-old adult heart. (B) Section at the level of the aortic sinus. Three leaflets of the aortic valve and one of the pulmonary valve are seen, with scattered labeled cells in the aortic leaflets and in the presumptive fibrous cardiac skeleton (examples of both indicated by arrowheads). Arrows point to labeled cells in the wall of the left coronary artery and of smaller coronary artery branch. The inset (B′) shows a higher magnification of the area indicated by the box in B, and illustrates the longitudinal organization of labeled cells in the wall of the proximal coronary artery, suggestive of a smooth muscle fate. (C) Section at the origin of the pulmonary arteries from the pulmonary trunk. A sharp boundary between labeled cells present in the PT and unlabeled cells in the pulmonary arteries is indicated by the arrows. The ligamentum arteriosum is strongly stained. The star at far left is placed in the wall of the ascending aorta. The left recurrent laryngeal nerve branches from the left vagus nerve underneath the ligamentum arteriosum; both nerves fibers carry parasympathetic nerves that are neural-crest-derived and stain positively. (D) Section through the right ventricular wall, indicating staining in a presumptive nerve fiber located within the epicardium (compare with A). (E) Section through the arch of the aorta at the origin of the unlabeled left subclavian artery. (F) Section through the right carotid and right subclavian arteries just anterior to the branchpoint of each from the innominate artery. The entire wall of the rca is labeled at this level, and a scattering of labeled cells (arrowheads) are seen in the wall of the rsca close to the innominate artery. Abbreviations: ligA, ligamentum arteriosum; n, left recurrent laryngeal nerve; RV inf, subvalvular infundibulum of the right ventricle; X, vagus nerve; other abbreviations are as in the legend to Fig. 4.

aortae. The subclavian arteries originate from the dorsal aortae in the caudalmost portion of the thoracic cavity (i.e., are not pharyngeal; Fig. 4F). Over time, these vessels migrate anteriorly, such that the right subclavian artery branches from the innominate artery and the left subclavian artery branches from the arch of the aorta opposite the ductus arteriosus. The early subclavian arteries and their origins in the dorsal aortae were never invested with neural crest and, in the final pattern, these vessels remain unlabeled, except for scattered cells located at the junction with the arch of the aorta (Figs 4K,L, 5A,E,F).

Neural-crest-derived cells can be seen migrating into the conotruncal region as early as E10.5 and, at E11.5, a broad patch of crest cells is diffusely present in and seems to constitute a significant portion of the conotruncal cushion mesenchyme. Beginning around E12.5, the outflow valves form at the junction of the conotruncal and aorticopulmonary septa. Labeled cells present in this region (Fig. 4A) assemble into the forming valve leaflets (Fig. 4C); however, the ultimate contribution of crest cells to the valves is not substantial in late embryos or in postnatal animals (Figs 4B,E, 5B). During late embryogenesis and in the newborn, a ribbon of labeled cells connects the pulmonary and aortic valves (Fig. 4A-C,E). This ribbon is derived from mesenchymal cells that populated the conotruncal septum at earlier stages, and is possibly part of the fibrous cardiac skeleton in later life. In the adult heart, scattered labeled cells occupy the fibrous region between the valves (Fig. 5B), but this contribution is limited.

The coronary arteries originate from the aorta just distal to the aortic valve and branch out to infiltrate the cardiac muscle. The proximal portion of the coronary arteries forms from a periaortic plexus of endothelium that penetrates into the aortic sinus and fuses with the aortic endothelium, whereas the distal coronary artery endothelium originates from cells that are initially found in the subepicardial space (Waldo et al., 1990). The smooth muscle wall of the coronary arteries is believed also to arise mostly from the subepicardial population (Mikawa and Gourdie, 1996). In late embryonic and neonatal Wnt1-Cre/R26R animals, an aggregation of labeled cells is found surrounding the aortic and pulmonary valves, and surrounding the origins of the coronary arteries (Fig. 4E). In the adult, these cells persist in the wall of the proximal coronary arteries and their immediate branches (Fig. 5B), and diminish in abundance with distance from the ascending aorta. Based on their morphological appearance and distribution, these labeled cells appear to be smooth muscle.

The pulmonary arteries form as sprouts that project from the proximal portions of the left and right sixth arch arteries towards the developing lung. At all stages from the time of their formation (Fig. 3D), the entirety of the pulmonary arterial walls are unlabeled and, at later stages, a very sharp line of labeled cells defines the junction between the pulmonary trunk and the pulmonary arteries (Figs 4I, 5C). This is somewhat surprising in that, at E10.5-12.0, crest cells seem plentiful in the region where the pulmonary arteries originate (Fig. 2H). Furthermore, crest cells line the wall of the pulmonary trunk both proximal and distal to the position of the pulmonary arteries at all stages. At E12.0, when the right sixth arch artery regresses, and when the nascent pulmonary arteries can first be observed histologically, the earlier density of crest cells in the surrounding mesenchyme has regressed. Presumably, the walls of the pulmonary arteries are derived from splanchnic mesoderm that surrounds the trachea and bronchi.

Labeled cells reflective of a neural crest origin were never seen in the atrial inflow region, in the atrial chambers, in the atrioventricular canal or in the mature mitral and tricuspid valves.

Neural crest contribution to organs in the vicinity of the developing heart

The thymus, thyroid and parathyroid organs are initially derived from outpocketings of the pharyngeal endoderm, which recruit pharyngeal mesenchyme cells as the organs differentiate. A functional role for cardiac neural crest cells in the establishment and differentiation of these organs has been inferred from anatomical (hypoplastic) deficiencies in these tissues following neural crest ablation in chick embryos (Bockman and Kirby, 1984; Kirby and Waldo, 1990), from mutation of the *Pax3* and *endothelin 1* genes in mice (Epstein et al., 1991; Kurihara et al., 1995a), and from physiological alterations seen in human DiGeorge syndrome patients (Greenberg, 1993).

The thymus originates from the lateral sides of the third pharyngeal pouch, and this area is invested with neural crest from the time of its formation (Fig. 2D). The thymic lobes are first recognizable in sections at E12.5, after they have severed their connection to the foregut and have descended to the superior mediastinum, where they are located immediately anterior to the arch of the aorta (Fig. 4G). As noted above, this is the period in development when the fairly diffuse mesenchymal staining pattern seen from earlier stages becomes condensed around the developing blood vessels and, similarly, the thymic lobes retain a circumferential ring of labeled cells in the posterior body wall at E12.5 and E13.5. The thymic lobes expand dramatically from E14.5 to the end of gestation, coincident with the onset of thymocyte production. Interestingly, through this later period, while labeled cells continue to occupy portions of the epithelial margin of the thymic lobes, particularly in the posterior region facing the pericardial cavity (Fig. 4I,J), most of the thymus is unlabeled, and the overall contribution of labeled cells to the newborn and adult thymus appears to be marginal if present at all.

The thyroid primordium is first recognizable at E9.5 as a bud (diverticulum) from the midline of the ventral foregut at the level of the second pharnygeal pouch (Fig. 2B). At the time of its appearance, the thyroid is surrounded by neural crest cells of second and third arch origin migrating between the foregut and the aortic sac. At E10.5, the thyroid has separated from the floor of the endoderm, is found anterior to the bifurcation of the third arch arteries from the aortic sac (the second arch arteries having regressed by this time), and remains surrounded by labeled mesenchymal cells (Fig. 2E). Similar to the thymus, the thyroid loses most if not all of its investment of neural crest cells as it assumes its final position flanking the trachea and becomes surrounded by splanchnic mesoderm (Fig. 4H). We cannot yet exclude the possibility that a scattered and numerically small population of labeled cells persists within the mature thyroid.

Similar to the thymus, the parathyroids also originate from the third pouch. It was not possible with the techniques used in the current study to identify the parathyroid organs and to follow the contribution of neural crest to their histogenesis.

An altered pattern of neural crest cells in an embryo with aortic arch artery malformation

In the course of this study, we recovered one embryo at E17.5 that had a congenital aortic arch artery malformation termed right-sided aortic arch. This phenotype involved the retention of the right fourth arch artery as the arch of the aorta, the right sixth arch artery as the ductus arteriosus, and the right dorsal aorta as the descending aorta. We have examined over 100 embryos from a similar strain and genetic background as this one embryo without ever observing any cardiovascular malformation, and so cannot account for the etiology of this case. Nonetheless, this embryo provides an interesting example of altered distribution of neural-crest-derived cells in a context where the normal fate of the aortic arch arteries is altered. Effectively, the distribution of labeled cells observed in this late-stage embryo was appropriate for the mature fate of each artery, even though the aortic arch arteries that were selected for preservation and reorganization into the mature pattern were not the normal ones. For example, the staining pattern observed around the right-sided ductus arteriosus in this embryo (Fig. 6) was typical of that seen in a normal left-sided ductus arteriosus (Fig. 4D), even though the right sixth arch artery should normally lose its investment of neural crest cells at E12.0 and regress. The expected staining pattern around the aorta and pulmonary trunk, and the absence of staining around the dorsal aorta and the pulmonary arteries, were normal in this embryo. This demonstrates that the fate of the aortic arch arteries and the cardiac neural crest cells are inter-related, although whether an alteration in crest cell distribution initiated the altered arterial pattern in this abnormal embryo, or whether the distribution of crest cells is responsive to an altered arterial pattern, cannot be determined at this time.

DISCUSSION

We have employed a two-component Cre/lox strategy to label neural crest progeny in mouse embryos and in postnatal stages. All tissues that were expected to be of neural crest origin were labeled at high if not complete efficiency and easily detected throughout development into adulthood. A conceptually similar approach as ours was recently described (Yamauchi et al., 1999), in which the P0 promoter was used to drive Cre expression, and with a conditional reporter gene driven by the chick β-actin promoter. That study described only incomplete expression of the reporter gene in neural-crest-derived tissues, and significant ectopic expression as well, indicating the importance of the correct components to achieve highly specific labeling with the Cre/lox strategy. The only obviously aberrant expression we have observed is an occasional labeling of a small cluster of cells in the ventricle (e.g., see Fig. 3A), the origin or fate of which we cannot explain. While the strategy that we describe offers distinct experimental advantages, it is appropriate to note that our approach is predicated on gene expression, and that experimental manipulations that alter or induce *Wnt1-Cre* expression or alter expression of the ROSA26 locus could give rise to an artifactual pattern.

Fig. 6. Neural crest cell fate in an embryo with an aortic arch artery malformation. In this embryo, the aorta and pulmonary trunk connect to the right dorsal aorta. Notice the staining pattern in the right-sided ductus arteriosus, which is appropriate for a left-sided DA, as well as the normal pattern in all other structures (compare to Fig. 4D). Abbreviations as in legend to Fig. 4.

Previous studies have utilized a number of methods to identify mouse cardiac neural crest cell progeny, although most have significant shortcomings and most do not label cells in the midgestation heart. A β-galactosidase transgene driven by a portion of the connexin 43 promoter (Lo et al., 1997) has come closest to replicating the pattern that we describe in this study; furthermore, the expression pattern of this transgene in the developing heart has been extensively compared to the distribution of avian neural crest cells in quail-chick chimeras (Waldo et al., 1999). Most features of the expression pattern that we observe with the *Wnt1-Cre*/R26R combination are in agreement with results from the avian studies and from the analysis of the *Cx43-lacZ* transgene, in particular during earlier aspects of cardiovascular development prior to overt septation (i.e., prior to E11.5 in the mouse). Thus, in all three models, labeled cells constitute the majority of the pharyngeal arch mesenchyme, display an abrupt transition at the junctions of the pharyngeal arch arteries with the dorsal aortae, and are not present in the subclavian or pulmonary arteries. Similarly, in all three models, labeled cells infiltrate between the foregut endoderm and the endothelium of the aortic sac, and then progress into the conotruncal cushions. The *Cx43-lacZ* transgene is ectopically expressed in pharyngeal ectoderm, but is otherwise consistent with the *Wnt1-Cre*/R26R expression pattern at these stages. During the initial stages of outflow tract septation, we observe much more extensive labeling in the forming aorticopulmonary septum (Fig. 3A) and in the mesenchyme of the conotruncal cushions (Figs 2F,G, 3A, 4A) than is seen with the *Cx43-lacZ* transgene, although the timing and pattern is comparable. Similarly, the refinement of the mesenchymal distribution into the subendocardial layer of the conotruncus (Fig. 3C), a process observed in avian chimeras, is also more prominent in our sections relative to the *Cx43-lacZ* transgene. The restricted location of neural crest progeny around the perimeter of the thymus (Fig. 4) is consistent with prior results from avian chimeras and the *Cx43-lacZ* transgene as well.

To a certain extent, some of the differences in staining between the two mouse models might represent experimental approaches: the Cx43-lacZ product is nuclear localized and was examined in 10 μm sections, whereas the R26R product is cytoplasmic and from E11.5 was examined in 20 μm sections. The visual impression of our sections might overemphasize the actual contribution of neural crest cells, particularly in the E11.5-12.5 conotruncal cushions where the apparent absence of unlabeled cells (Figs 3A, 4A) is clearly at odds with the known substantial contribution of endothelial-derived cell populations. At the same time, it is also likely that the Cx43-lacZ transgene stains only a subpopulation of neural crest cells, particularly at E12.5 and later, where the number

of labeled cells decreases relative to what is expected from avian chimeras and relative to the *Wnt1-Cre*/R26R pattern. This is almost certainly an indication of reduced Cx43 promoter activity as the neural-crest-derived mesenchymal cells assume differentiated fates. One of the strengths of our approach is that the long-term fate of neural crest cells can be discerned in late gestation and in postnatal tissues, regardless of the phenotype of these cells. Thus, the extensive neural crest contribution that we observe to the ductus arteriosus and the arch of the aorta, and to the carotid and innominate arteries, is consistent with avian studies and is only suggested by the *Cx43-lacZ* transgene expression pattern. Similarly, the presence of neural-crest-derived cells in the leaflets of the mammalian outflow valves (Figs 4E, 5B), in the subvalvular conus facing the ventricular septum (Fig. 4B,C), and in the walls of the ascending aorta and pulmonary trunk is consistent with avian studies, and mostly unobserved with the *Cx43-lacZ* transgene.

A novel and unexpected observation made in this study is a contribution of neural crest progeny to the walls of the proximal coronary arteries. We observe a substantial mesenchymal neural crest population in the vicinity of the truncus arteriosus (Fig. 3A), from which the outflow valves will form, and can follow these labeled cells as they become incorporated into the nascent coronary arteries and outflow valve leaflets (Figs 4E, 5B). The contribution of labeled cells to the walls of the coronary arteries decreases with distance from the ascending aorta. The smooth muscle lining of the coronary arteries in avian embryos has previously been described as originating entirely from the epicardium, without a neural crest contribution. Possibly, the relatively small contribution that we describe here was overlooked in the avian studies, or perhaps the mouse and avian embryos differ in this regard.

Because our approach results in the marking of all neural crest cell lineages, we cannot define the axial level from which the labeled cells that we observe in the heart outflow region originate. At E9.5, cells in the truncus arteriosus and aortic sac are almost certainly derived from the third pharyngeal arch; however, when the fourth and sixth arches form, the relative contributions of crest cells to the heart from each arch cannot be defined. Previous studies in which the lineage tracer DiI has been injected into embryos cultured in vitro have not been very successful in labeling cells in the heart. Possibly, the best way to address this problem will be to cross the *Wnt1-Cre* and R26R genes into mutant backgrounds in which specific arch derivatives are believed to be compromised. For example, the *HoxA3* mutation results in thymic and thyroid defects, but not vessel abnormalities (Manley and Capecchi, 1995), consistent with an effect specifically on the third arch, whereas a recently described mouse chromosome 16 deletion, which causes vessel abnormalities but does not cause thymic, thyroid or parathyroid deficiencies (Lindsay et al., 1999), is proposed to specifically affect the fourth arch.

A significant body of experimental analysis has led to the conclusion that the cardiac neural crest population has a critical role in the reorganization of the pharyngeal arch arteries. It is interesting that the distribution of neural crest cells does not provide an explanation for this role, i.e., of the several morphogenic processes that occur during pharyngeal arch artery remodeling, in no case does a redistribution of neural crest cells presage these events. Rather, morphogenic alterations occur simultaneous to an alteration of neural crest cell pattern (i.e., the regression of the right sixth arch artery at E12.0), without any recognizable alteration in crest cell distribution (i.e., the bilateral regression of the first and second arch arteries by E10.5), or occur at more caudal levels where neural crest cells are not found (i.e., regression of the posterior part of the right dorsal aorta and anterior migration of the subclavian arteries by E12.5). Thus, the mere presence or absence of crest cells is not sufficient to cause these events.

In contrast, as evidenced from neural-crest-ablated chick embryos, neural crest is required for elaboration of the conotruncal septum. The extensive distribution of mammalian neural crest cells prior to (Fig. 3) and shortly following (Fig. 4A-C) septation supports such a role. Nonetheless, the ultimate contribution of neural crest to the subvalvular region of the outflow tract is negligible and to the valvular region is scant. Somewhat similarly, the extensive staining of the aorticopulmonary septum is mostly lost as the ascending aorta and pulmonary trunk mature, retaining a thin subendothelial band of neural-crest-derived smooth muscle tissue in the immediate supravalvular region.

It is apparent from this study that the distribution of mammalian neural crest cells in the pharyngeal and cardiac region is dynamic over time, in general progressing from a widespread mesenchymal distribution to a much more tightly focused localization. We cannot define whether the refinement of crest cell pattern results from cell death, cell migration or differential proliferation with respect to neighboring non-crest mesenchyme. Furthermore, we cannot determine from the mature pattern whether or how the crest cell population might have influenced earlier morphogenic events. For example, neural crest cells seem to represent a trivial percentage of the cells in the postnatal thymus and thyroid, yet might play an essential role in the genesis of these structures much earlier when these organ primordia were enveloped by crest cells. Similarly, the limited representation of crest cells in the conotruncal septum of the mature heart is almost certainly at odds with a crucial role in conotruncal septation at E11.5-12.5, when the crest cell population is far more numerous.

The neural crest has fascinated developmental biologists for over 100 years (Hall and Horstadius, 1988). The highly efficient, specific and permanent marking of mouse neural crest progeny as described in this and the accompanying (Chai et al., 2000) report will facilitate new experimental approaches in the analysis of the fate and function of the mammalian neural crest.

The authors are grateful for the comments and suggestions of Margaret Kirby and Karen Waldo during the preparation of this manuscript. This work was supported by a Grant-in-Aid from the national center of the American Heart Association, and by a Cardiovascular Research Development Award from the Los Angeles and Western States affiliate of the American Heart Association, to H. M. S.

REFERENCES

Bockman, D. E. and Kirby, M. L. (1984). Dependence of thymus development on derivatives of the neural crest. *Science* **223,** 498-500.

Chai, Y., Jiang, X., Ito, Y., Bringas, P., Han, J., Rositch, D. H., Soriano, P., McMahon, A. P. and Sucov, H. M. (2000). Fate of the mammalian

cranial neural crest during tooth and mandibular morphogenesis. *Development* **127,** 1671-1679.

Conway, S. J., Henderson, D. J. and Copp, A. J. (1997). Pax3 is required for cardiac neural crest migration in the mouse: evidence from the splotch (Sp2H) mutant. *Development* **124,** 505-514.

Danielian, P. S., Muccino, D., Rowitch, D. H., Michael, S. K. and McMahon, A. P. (1998). Modification of gene activity in mouse embryos in utero by a tamoxifen-inducible form of Cre recombinase. *Current Biol.* **8,** 1323-1326.

Echelard, Y., Vassileva, G. and McMahon, A. P. (1994). Cis-acting regulatory sequences governing Wnt-1 expression in the developing mouse CNS. *Development* **120,** 2213-2224.

Epstein, D. J., Vekemans, M. and Gros, P. (1991). Splotch (Sp2H), a mutation affecting development of the mouse neural tube, shows a deletion within the paired homeodomain of Pax-3. *Cell* **67,** 767-774.

Fananapazir, K. and Kaufman, M. H. (1988). Observations on the development of the aortico-pulmonary spiral septum in the mouse. *J. Anat.* **158,** 157-72.

Franz, T. (1989). Persistent truncus arteriosus in the Splotch mutant mouse. *Anat. Embryol.* **180,** 457-464.

Friedrich, G. and Soriano, P. (1991). Promoter traps in embryonic stem cells: a genetic screen to identify and mutate developmental genes in mice. *Genes Dev.* **5,** 1513-1523.

Fukiishi, Y. and Morriss-Kay, G. M. (1992). Migration of cranial neural crest cells to the pharyngeal arches and heart in rat embryos. *Cell Tissue Res.* **268,** 1-8.

Greenberg, F. (1993). DiGeorge syndrome: an historical review of clinical and cytogenetic features. *J. Med. Genet.* **30,** 803-806.

Hall, B. K. and Horstadius, S. (1988). *The Neural Crest*. London: Oxford University Press.

Kaufman, M. H. (1992). *The Atlas of Mouse Development.* London: Harcourt Brace Jovanovich Academic Press.

Kirby, M. L., Gale, T. F. and Stewart, D. E. (1983). Neural crest cells contribute to normal aorticopulmonary septation. *Science* **220,** 1059-1061.

Kirby, M. L. and Waldo, K. L. (1990). Role of neural crest in congenital heart disease. *Circulation* **82,** 332-340.

Kurihara, Y., Kurihara, H., Maemura, K., Kuwaki, T., Kumada, M. and Yazaki, Y. (1995a). Impaired development of the thyroid and thymus in endothelin-1 knockout mice. *J. Cardiovasc. Pharmacol.* **26 Supplement 3,** S13-16.

Kurihara, Y., Kurihara, H., Oda, H., Maemura, K., Nagai, R., Ishikawa, T. and Yazaki, Y. (1995b). Aortic arch malformations and ventricular septal defect in mice deficient in endothelin-1. *Journal of Clinical Investigation* **96,** 293-300.

Lammer, E. J., Chen, D. T., Hoar, R. M., Agnish, N. D., Benke, P. J., Braun, J. T., Curry, C. J., Fernhoff, P. M., Grix, A. W., Lott, I. T., Richard, J. M. and Sun, S. C. (1985). Retinoic acid embryopathy. *N. Engl. J. Med.* **313,** 837-841.

Le Lievre, C. S. and LeDouarin, N. M. (1975). Mesenchymal derivatives of the neural crest. Analysis of chimaeric quail and chick embryos. *J. Embryol. Exp. Morph.* **34,** 125-154.

LeDouarin, N. M. (1982). *The Neural Crest.* Cambridge: Cambridge Univ. Press.

Lee, R. Y., Luo, J., Evans, R. M., Giguere, V. and Sucov, H. M. (1997). Compartment-selective sensitivity of cardiovascular morphogenesis to combinations of retinoic acid receptor gene mutations. *Circ. Res.* **80,** 757-764.

Lindsay, E. A., Botta, A., Jurecic, V., Carattini-Rivera, S., Cheah, Y.-C., Rosenblatt, H. M., Bradley, A. and Baldini, A. (1999). Congenital heart disease in mice deficient for the DiGeorge syndrome region. *Nature* **401,** 379-383.

Liu, Y. H., Ma, L., Wu, L. Y., Luo, W., Kundu, R., Sangiorgi, F., Snead, M. L. and Maxson, R. (1994). Regulation of the Msx2 homeobox gene during mouse embryogenesis: a transgene with 439 bp of 5′ flanking sequence is expressed exclusively in the apical ectodermal ridge of the developing limb. *Mech. Dev.* **48,** 187-97.

Lo, C. W., Cohen, M. F., Huang, G. Y., Lazatin, B. O., Patel, N., Sullivan, R., Pauken, C. and Park, S. M. (1997). Cx43 gap junction gene expression and gap junctional communication in mouse neural crest cells. *Dev. Genet.* **20,** 119-132.

Manley, N. R. and Capecchi, M. R. (1995). The role of Hoxa-3 in mouse thymus and thyroid development. *Development* **121,** 1989-2003.

Means, A. L. and Gudas, L. J. (1997). The CRABP I gene contains two separable, redundant regulatory regions active in neural tissues in transgenic mouse embryos. *Dev. Dynam.* **209,** 59-69.

Mikawa, T. and Gourdie, R. G. (1996). Pericardial mesoderm generates a population of coronary smooth muscle cells migrating into the heart along with ingrowth of the epicardial organ. *Dev. Biol.* **174,** 221-232.

Miyagawa-Tomita, S., Waldo, K., Tomita, H. and Kirby, M. L. (1991). Temporospatial study of the migration and distribution of cardiac neural crest in quail-chick chimeras. *Am. J. Anat.* **192,** 79-88.

Nakajima, Y., Krug, E. L. and Markwald, R. R. (1994). Myocardial regulation of transforming growth factor-beta expression by outflow tract endothelium in the early embryonic chick heart. *Dev. Biol.* **165,** 615-626.

Serbedzija, G. N., Bronner, F. M. and Fraser, S. E. (1992). Vital dye analysis of cranial neural crest cell migration in the mouse embryo. *Development* **116,** 297-307.

Soriano, P. (1999). Generalized lacZ expression with the ROSA26 Cre reporter strain. *Nature Genetics* **21,** 70-71.

van den Hoff, M. J., Moorman, A. F., Ruijter, J. M., Lamers, W. H., Bennington, R. W., Markwald, R. R. and Wessels, A. (1999). Myocardialization of the cardiac outflow tract. *Dev. Biol.* **212,** 477-490.

Waldo, K., Miyagawa, T. S., Kumiski, D. and Kirby, M. L. (1998). Cardiac neural crest cells provide new insight into septation of the cardiac outflow tract: aortic sac to ventricular septal closure. *Dev. Biol.* **196,** 129-144.

Waldo, K. L., Lo, C. W. and Kirby, M. L. (1999). Connexin 43 expression reflects neural crest patterns during cardiovascular development. *Dev. Biol.* **208,** 307-323.

Waldo, K. L., Willner, W. and Kirby, M. L. (1990). Origin of the proximal coronary artery stems and a review of ventricular vascularization in the chick embryo. *Am. J. Anat.* **188,** 109-120.

Wilson, J. G. and Warkany, J. (1949). Aortic arch and cardiac anomalies in the offspring of vitamin A deficient rats. *Am. J. Anat.* **85,** 113-155.

Yamauchi, Y., Abe, K., Mantani, A., Hitoshi, Y., Suzuki, M., Osuzu, F., Kuratani, S. and Yamamura, K. (1999). A novel transgenic technique that allows specific marking of the neural crest cell lineage in mice. *Dev. Biol.* **212,** 191-203.

Zambrowicz, B. P., Imamoto, A., Fiering, S., Herzenberg, L. A., Kerr, W. G. and Soriano, P. (1997). Disruption of overlapping transcripts in the ROSA beta geo 26 gene trap strain leads to widespread expression of beta-galactosidase in mouse embryos and hematopoietic cells. *Proc. Natn. Acad. Sci. USA* **94,** 3789-3794.

Note added in proof

An earlier publication described a similar technical approach to fate mapping of cells in the Wnt1 expression domain: Dymecki, S. M. and Tomasiewicz, H. (1998). Using Flp-recombinase to characterize expansion of Wnt1-expressing neural progenitors in the mouse. *Dev. Biol.* **201**, 57-65.